A General Technique for Eliminating Spurious Oscillations in Conservative Schemes for Multiphase and Multispecies Euler Equations *

Ronald P. Fedkiw † Xu-Dong Liu ‡ Stanley Osher §

September 1, 2000

Abstract

Standard conservative discretizations of the compressible Euler equations have been shown to admit nonphysical oscillations near some material interfaces. For example, the calorically perfect Euler equations admit these oscillations when both temperature and gamma jump across an interface, but not when either temperature or gamma happen to be constant. These nonphysical oscillations can be alleviated to some degree with a nonconservative modification of the total energy computed by solving a coupled evolution equation for the pressure. In this paper, we develop and illustrate this method for the thermally perfect Euler equations.

^{*}Research supported in part by ONR N00014-97-1-0027, ARPA URI-ONR-N00014-92-J-1890, NSF $\#\mathrm{DMS}$ 94-04942, and ARO DAAH04-95-1-0155

[†]Computer Science Department, Stanford University, Stanford, California 94305. Email: fedkiw@cs.stanford.edu

[‡]Department of Mathematics, University of California Santa Barbara, Santa Barbara, California 93106. Email: xliu@math.ucsb.edu

[§]Department of Mathematics, University of California Los Angeles, Los Angeles, California 90095. Email: sjo@math.ucla.edu

1 Introduction

Fully conservative numerical methods have been shown to admit nonphysical oscillations near material interfaces, e.g. see [7] and [6]. In [5], fully conservative discretization of the calorically perfect Euler equations was shown to admit these nonphysical oscillations when there is a jump in both temperature and gamma across an interface, but not when either temperature or gamma happen to be constant. [6] and [5] propose nonconservative modifications of the fully conservative numerical method in regions where difficulties may occur. These modifications give rise to conservation errors in the total energy of the system, and thus yield a locally nonconservative formulation. In general, nonconservative formulations give the wrong shock speeds, although the errors in shock speeds can be reduced significantly if a special viscosity term is added, see [8]. [6] and [5] do not make use of this special viscosity term, however, their numerical methods are fully conservative except on a set of measure zero under grid refinement and seem to produce adequate shock speeds.

In [6], the examples seem to indicate that the mass fraction formulation is nearly adequate in the fully conservative framework, while the level set formulation (used carelessly) admits wild nonphysical oscillations on the same problems. The cause of these oscillations for level set methods stems back to [9] where the authors used the level set formulation in order to reconstruct gamma as a perfect Heaviside function even though the density was numerically smeared out. In fact, [1] shows that it is important for gamma to have a special smeared out numerical profile near the discontinuity in order to alleviate nonphysical oscillations. More recently, [10], [11] and [12] have extended the seminal work in [1]. Using ideas from [1] most of the large oscillations in the level set calculations of [6] can be removed producing results comparable with the the mass fraction formulations in [6].

We follow along the lines of [6] and [5] formulating the problem in a conservative fashion, only applying the nonconservative method as a local correction to an existing conservative solver. Our nonconservative correction method is based on the approach in [6].

2 Euler Equations

Consider the two dimensional thermally perfect Euler Equations for multispecies flow with a total of N species,

$$\vec{U}_t + [\vec{F}(\vec{U})]_x + [\vec{G}(\vec{U})]_y = 0, \tag{1}$$

$$\vec{U} = \begin{pmatrix} \rho \\ \rho u \\ \rho v \\ E \\ \rho Y_1 \\ \vdots \\ \rho Y_{N-1} \end{pmatrix}, \quad \vec{F}(\vec{U}) = \begin{pmatrix} \rho u \\ \rho u^2 + p \\ \rho u v \\ (E+p)u \\ \rho u Y_1 \\ \vdots \\ \rho u Y_{N-1} \end{pmatrix}, \quad \vec{G}(\vec{U}) = \begin{pmatrix} \rho v \\ \rho u v \\ \rho v^2 + p \\ (E+p)v \\ \rho v Y_1 \\ \vdots \\ \rho v Y_{N-1}, \end{pmatrix} (2)$$

$$E = \rho e + \frac{\rho(u^2 + v^2)}{2}, \qquad h = e + \frac{p}{\rho}$$
 (3)

$$h = \sum_{i=1}^{N} Y_i h_i(T), \qquad h_i(T) = h_i^f + \int_0^T c_{p,i}(s) ds$$
 (4)

where t is time, x and y are the spatial dimensions, ρ is the density, u and v are the velocities, E is the energy per unit volume, Y_i is the mass fraction of species i, e is the internal energy per unit mass, h is the enthalpy per unit mass, p is the pressure, h_i is the enthalpy per unit mass of species i, h_i^f is the heat of formation of species i (enthalpy at 0K), T is the temperature, and $c_{p,i}$ is the specific heat at constant pressure of species i. Note that $Y_N = 1 - \sum_{i=1}^{N-1} Y_i$. Note that the pressure is a function of the density, internal energy per unit mass, and the mass fractions, $p = p(\rho, e, Y_1, \dots, Y_{N-1})$. See [3] for more details.

3 Pressure Evolution Equation

In order to apply a nonconservative correction to the total energy, [6] solves a partial differential equation for the pressure. Here, we state this equation for the general equation of state $p = p(\rho, e, Y_1, \dots, Y_{N-1})$ with partial derivatives denoted by p_{ρ} , p_e and p_{Y_i} . The convective derivative of the pressure

$$\frac{Dp}{Dt} = p_{\rho} \frac{D\rho}{Dt} + p_{e} \frac{De}{Dt} + \sum_{i=1}^{N-1} \left(p_{Y_{i}} \frac{DY_{i}}{Dt} \right)$$
 (5)

can be rewritten as

$$p_t + \vec{u} \cdot \nabla p = -\rho c^2 \nabla \cdot \vec{u} \tag{6}$$

using

$$\rho_t + \vec{u} \cdot \nabla \rho = -\rho \nabla \cdot \vec{u} \tag{7}$$

$$u_t + \vec{u} \cdot \nabla u = -\frac{p_x}{\rho} \tag{8}$$

$$v_t + \vec{u} \cdot \nabla v = -\frac{p_y}{\rho} \tag{9}$$

$$e_t + \vec{u} \cdot \nabla e = -\frac{p}{\rho} \nabla \cdot \vec{u} \tag{10}$$

and

$$(Y_i)_t + \vec{u} \cdot \nabla Y_i = 0 \tag{11}$$

which are all derived from the Euler equations in the previous section. Note that $\vec{u}=< u, v>$ is the velocity vector and $c=\sqrt{p_\rho+\frac{p}{\rho^2}p_e}$ is the speed of sound.

In some formulations of the equation of state, the pressure can depend on the level set function, ϕ , or on gamma, γ . Since both the level set function and gamma have a vanishing convective derivative,

$$\phi_t + \vec{u} \cdot \nabla \phi = 0 \tag{12}$$

$$\gamma_t + \vec{u} \cdot \nabla \gamma = 0 \tag{13}$$

they both drop out of the pressure evolution equation, similar to Y_i , leaving equation 6 unchanged.

Note that the pressure evolution equation reduces to the more familiar form

$$p_t + \vec{u} \cdot \nabla p = -\gamma p \nabla \cdot \vec{u} \tag{14}$$

when $c = \sqrt{\frac{\gamma p}{\rho}}$.

To obtain an upwind discretization of equation 6, we rewrite it as the last equation of a quasilinear system,

$$\begin{pmatrix} u \\ v \\ p \end{pmatrix}_t + \begin{pmatrix} u & 0 & \frac{1}{\rho} \\ 0 & u & 0 \\ \rho c^2 & 0 & u \end{pmatrix} \begin{pmatrix} u \\ v \\ p \end{pmatrix}_x + \begin{pmatrix} v & 0 & 0 \\ 0 & v & \frac{1}{\rho} \\ 0 & \rho c^2 & v \end{pmatrix} \begin{pmatrix} u \\ v \\ p \end{pmatrix}_y = 0 \quad (15)$$

where the eigenvalues and eigenvectors for the 3 by 3 matrix associated with convection in the x-direction are

$$\lambda_x^1 = u - c, \quad \lambda_x^2 = u, \quad \lambda_x^3 = u + c \tag{16}$$

$$\vec{L}_x^1 = \left(\frac{1}{2}, 0, \frac{-1}{2\rho c}\right), \quad \vec{L}_x^2 = (0, 1, 0), \quad \vec{L}_x^3 = \left(\frac{1}{2}, 0, \frac{1}{2\rho c}\right)$$
 (17)

$$\vec{R}_x^1 = \begin{pmatrix} 1 \\ 0 \\ -\rho c \end{pmatrix}, \quad \vec{R}_x^2 = \begin{pmatrix} 0 \\ 1 \\ 0 \end{pmatrix}, \quad \vec{R}_x^3 = \begin{pmatrix} 1 \\ 0 \\ \rho c \end{pmatrix}$$
 (18)

and the eigenvalues and eigenvectors for the 3 by 3 matrix associated with convection in the y-direction are

$$\lambda_y^1 = v - c, \quad \lambda_y^2 = v, \quad \lambda_y^3 = v + c \tag{19}$$

$$\vec{L}_y^1 = \left(0, \frac{1}{2}, \frac{-1}{2\rho c}\right), \quad \vec{L}_y^2 = (1, 0, 0), \quad \vec{L}_y^3 = \left(0, \frac{1}{2}, \frac{1}{2\rho c}\right) \tag{20}$$

$$\vec{R}_y^1 = \begin{pmatrix} 0 \\ 1 \\ -\rho c \end{pmatrix}, \quad \vec{R}_y^2 = \begin{pmatrix} 1 \\ 0 \\ 0 \end{pmatrix}, \quad \vec{R}_y^3 = \begin{pmatrix} 0 \\ 1 \\ \rho c \end{pmatrix}. \tag{21}$$

These eigensystems allow us to rewrite equation 15 as

$$\begin{pmatrix} u \\ v \\ p \end{pmatrix}_t + \sum_{i=1}^3 \left(\lambda_x^i \vec{R}_x^i \vec{L}_x^i \right) \begin{pmatrix} u \\ v \\ p \end{pmatrix}_x + \sum_{i=1}^3 \left(\lambda_y^i \vec{R}_y^i \vec{L}_y^i \right) \begin{pmatrix} u \\ v \\ p \end{pmatrix}_y = 0 \qquad (22)$$

so that each of the 6 terms can be upwinded according to the sign of the eigenvalue in that term.

The last equation in 22 is equivalent to equation 6, with p_x , u_x , p_y , and v_y replaced by

$$p_x = \frac{1}{2} \left(p_x^{u-c} + p_x^{u+c} \right) - \frac{\rho c}{2} \left(u_x^{u-c} - u_x^{u+c} \right)$$
 (23)

$$u_x = \frac{1}{2} \left(u_x^{u-c} + u_x^{u+c} \right) - \frac{1}{2\rho c} \left(p_x^{u-c} - p_x^{u+c} \right)$$
 (24)

$$p_y = \frac{1}{2} \left(p_y^{v-c} + p_y^{v+c} \right) - \frac{\rho c}{2} \left(v_y^{v-c} - v_y^{v+c} \right)$$
 (25)

$$v_y = \frac{1}{2} \left(v_y^{v-c} + v_y^{v+c} \right) - \frac{1}{2\rho c} \left(p_y^{v-c} - p_y^{v+c} \right)$$
 (26)

where the superscript on each spatial partial derivative refers to the eigenvalue which determines the upwind direction for the discretization of that spatial partial derivative. For example, p_x^{u-c} is the spatial derivative of the pressure discretized using the eigenvalue u-c to determine the upwind direction. A positive eigenvalue indicates characteristic information coming from the left, while a negative eigenvalue indicates characteristic information coming from the right. If an eigenvalue is identically zero, then equation 22 illustrates that the spatial derivative does not contribute to the solution, and can be assigned a zero value for practical purposes.

Note that in the case where the eigenvalues agree on the upwind direction (supersonic flow), the two separate spatial derivatives in each set of parenthesis coalesce into a single value. Thus, the second term in each equation vanishes, and equations 23 to 26 merely dictate upwind differencing in the obvious direction.

Note that we do not use the special viscosity discussed in [8], although it could be added to the quasilinear system, and the resulting system could be discretized in a fashion similar to that outlined above.

4 Modification of the Conservative Solver

In order to solve the two dimensional Euler equations, we utilize a fully conservative high order accurate algorithm as outlined in [3] and [4], along with the Complementary Projection Method in [2] which gives an efficient method for eigensystem treatment with no loss of accuracy. While adequate for many problems, the conservative solver occasionally admits large non-physical oscillations, and a nonconservative correction to the total energy needs to be applied in these regions.

Given an acceptable smooth solution for the conserved variables and the pressure given by the equation of state, the fully conservative numerical method computes new values for the conserved variables which can be used to find the new pressure again from the equation of state. It is this new pressure that causes the oscillations in regions where the interface is numerically problematic. An alternative pressure can be obtained from the pressure evolution equation, and this new pressure can be used to define a nonconservative energy using the equation of state. Then in regions where the interface is numerically problematic, the energy computed with the fully conservative numerical method is replaced with the nonconservative energy computed using the pressure evolution equation.

There are many way to locate potentially problematic interfaces. [6] uses jumps in the mass fraction and sign changes in the level set function. [5] looks for regions where both temperature and gamma change sign. In general, this procedure is dependent on the formulation of the problem, and one may want to consider many things, e.g. mass fractions, level sets, gamma, temperature, and equations of state. We recommend that the fully conservative solution be compared with the nonconservatively corrected solution in order to determine which flow features are physically authentic.

5 Numerical Examples

5.1 Example 1

Consider an isolated contact discontinuity separating oxygen and argon. Initially, velocity, pressure, and density are set to constant values while temperature has a jump across the contact discontinuity. The conservative scheme admits nonphysical oscillations as shown in figure 1. Application of a local nonconservative correction to the total energy alleviates these oscillations as shown in figure 2. The local correction was applied to about 3 to 5 grid points in the vicinity of the contact discontinuity.

5.2 Example 2

Consider a one dimensional shock tube problem with argon on the left and oxygen on the right. Both gases are initially at rest with a jump in both pressure and temperature across the interface initiating the formation of three waves: a shock wave, a contact discontinuity and a rarefaction wave. The fully conservative method admits small nonphysical oscillations as shown in figure 3 which are fixed by the nonconservative correction method in figure 4. The conservative scheme is adequate, although the nonconservative correction method gives smoother results near the contact discontinuity. Note that both schemes have a little trouble with the rarefaction corner. More importantly, note that the spike in energy is present in both schemes, and that it appears to be an authentic feature under grid refinement for the fully conservative scheme even though it lacks any physical relevance.

5.3 Example 3

A shock tube is placed at x=.4 and a contact discontinuity with a temperature jump is placed at x=.6. Oxygen gas is located to the left of x=.6 and argon gas is located to the right. The shock wave generated by the shock tube travels to the right and hits the interface at x=.6. Figure 5 shows the computed solution computed with the fully conservative method at a time where the shock wave has passed through the interface. Figure 6 shows the solution obtained using the nonconservative correction method. Comparison of figures 5 and 6 indicate that the conservative method admits large nonphysical oscillations. The nonconservative correction method performs much better, although there are still some imperfections in the

solution. Figures 7 and 8 show the computed results for a similar problem with different initial conditions.

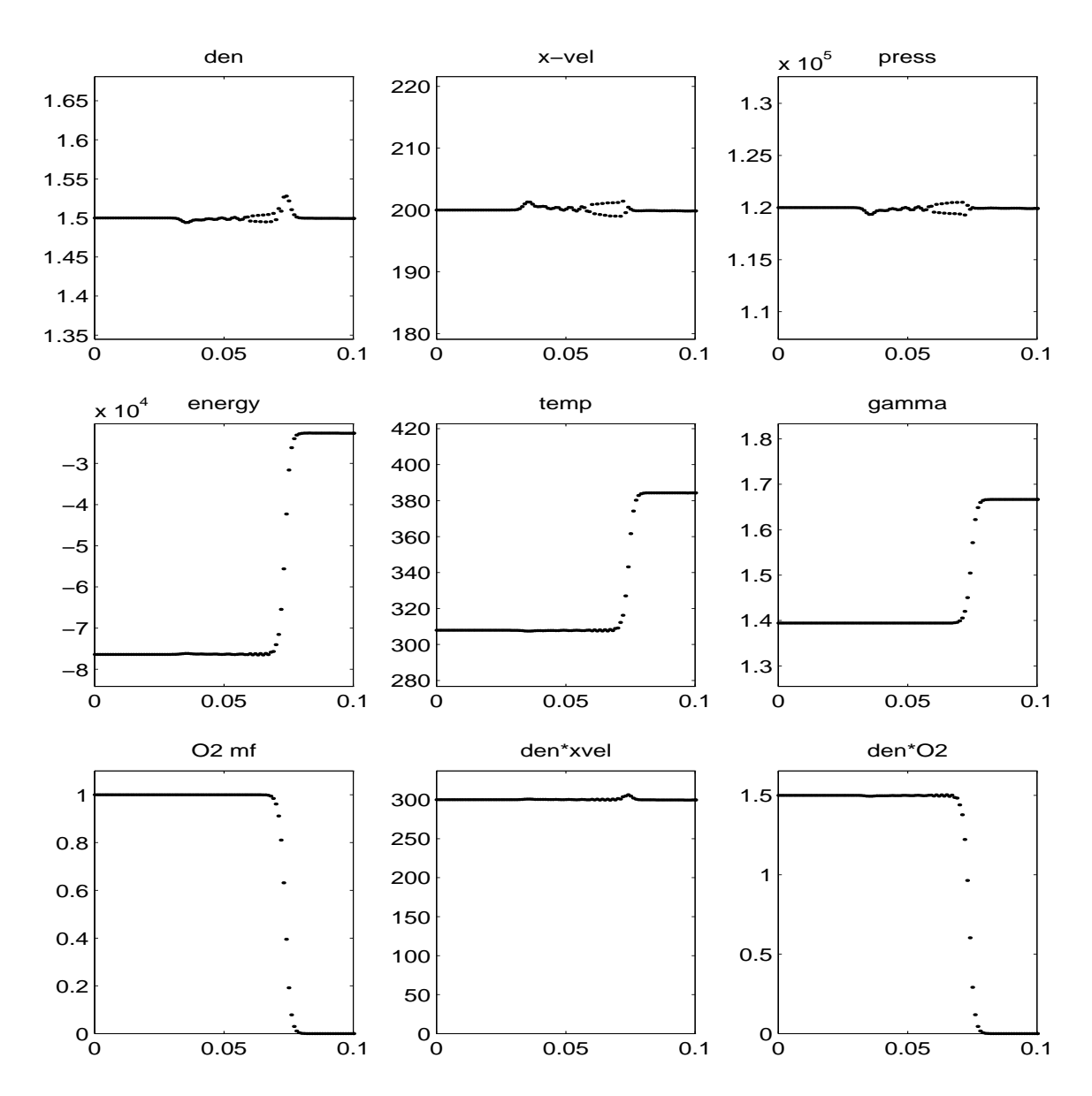


Figure 1: conservative method - contact discontinuity

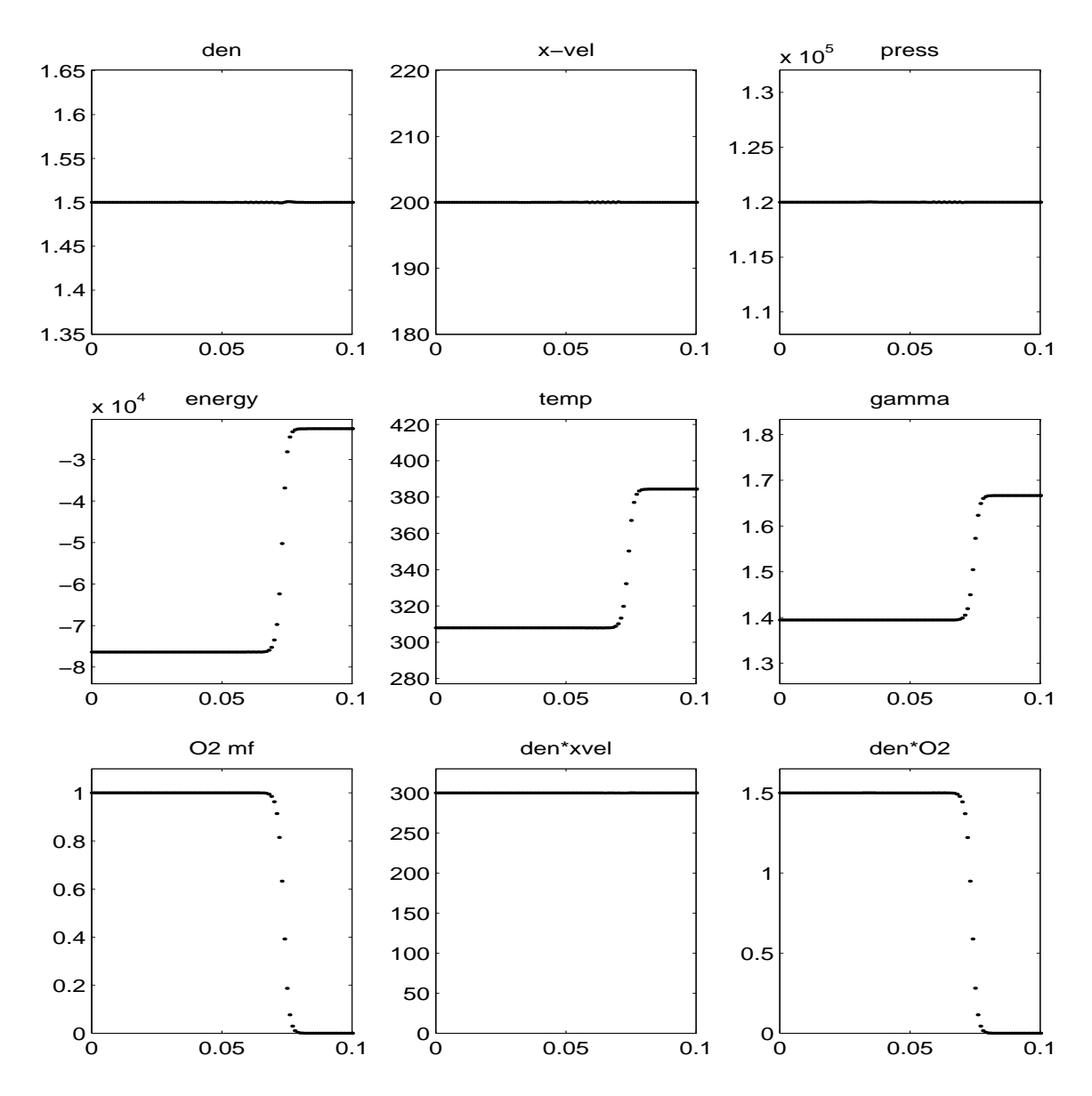


Figure 2: nonconservative correction - contact discontinuity

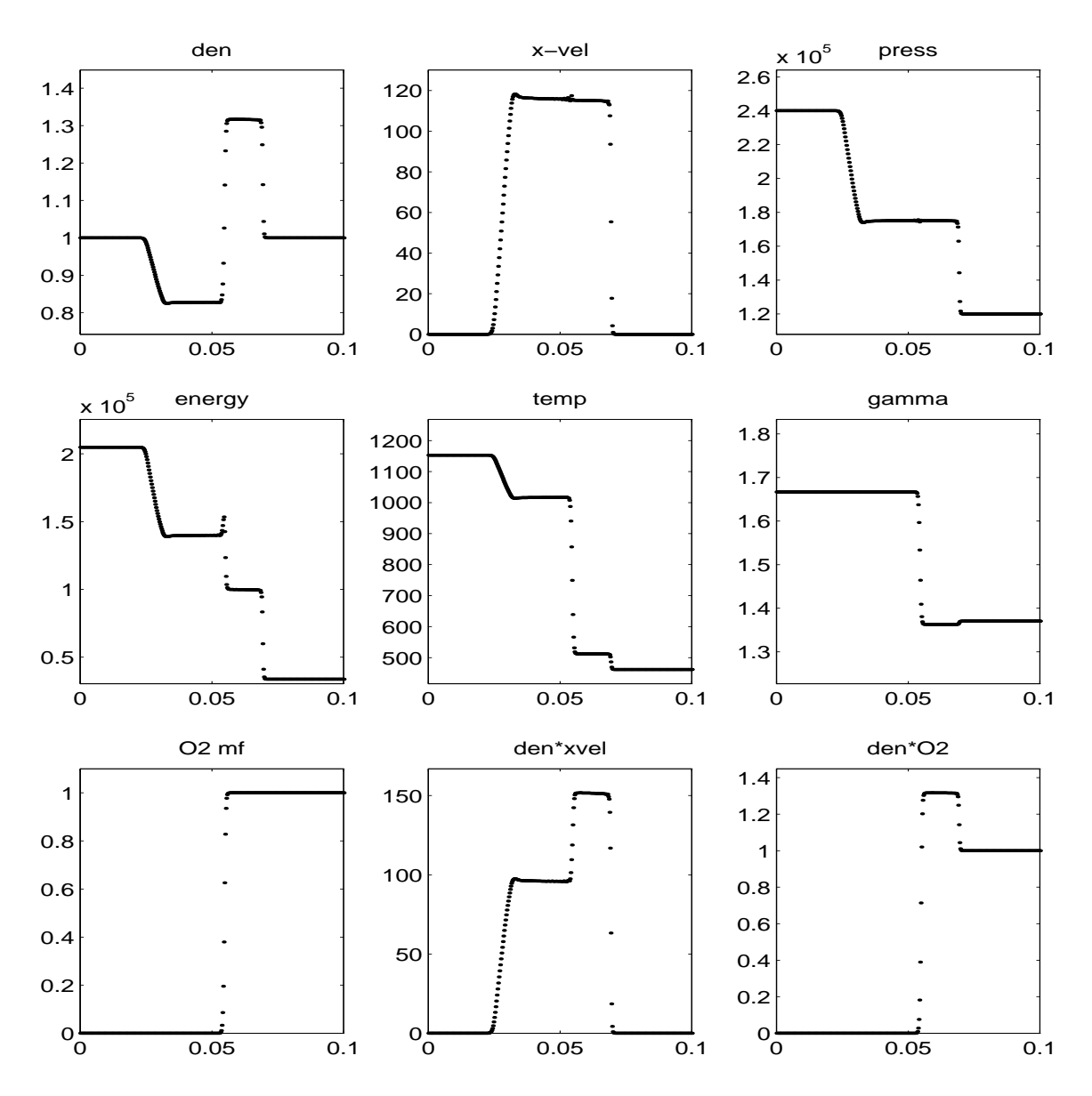


Figure 3: conservative method - shock tube - 400 points

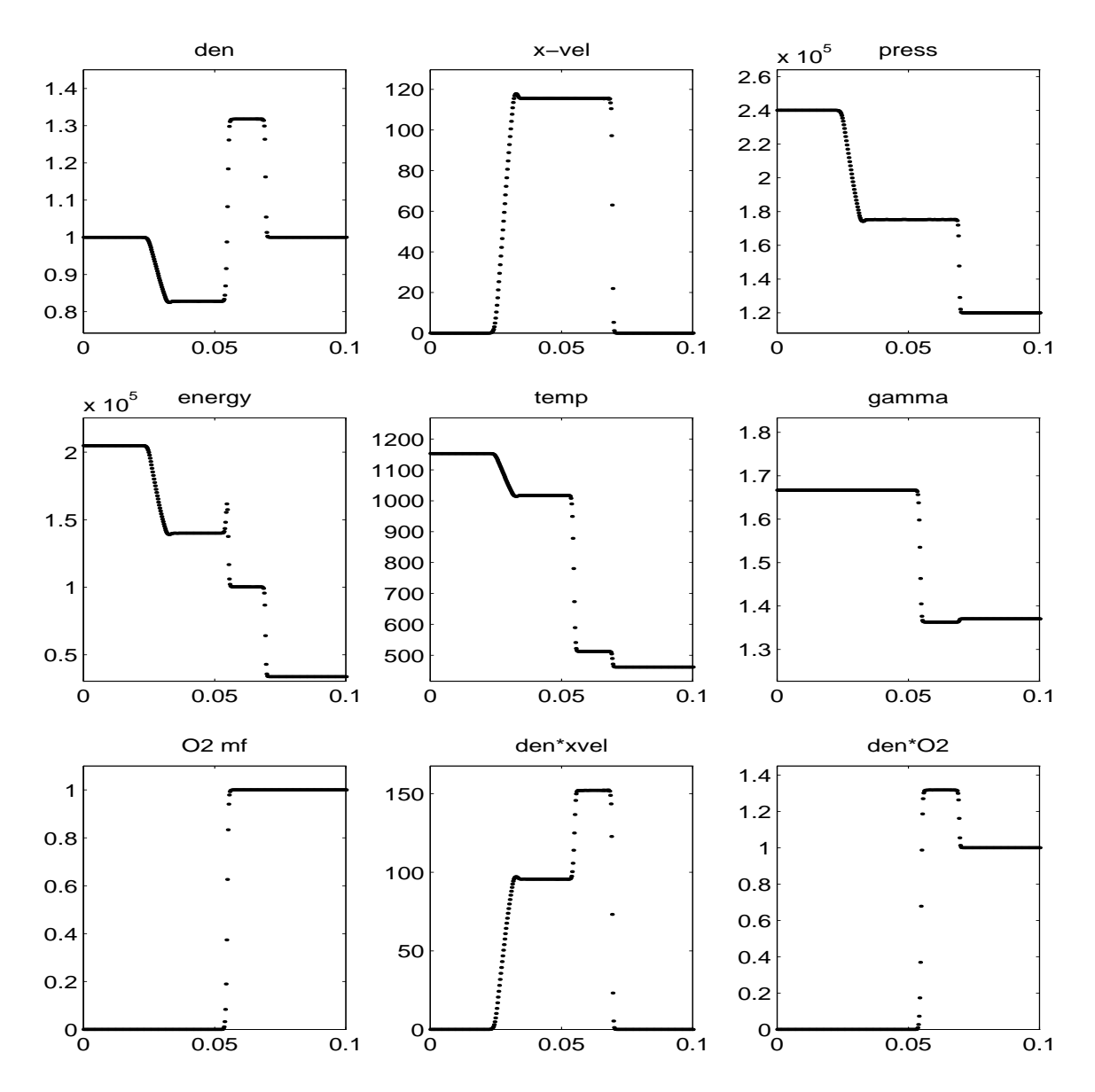


Figure 4: nonconservative correction - shock tube - 400 points

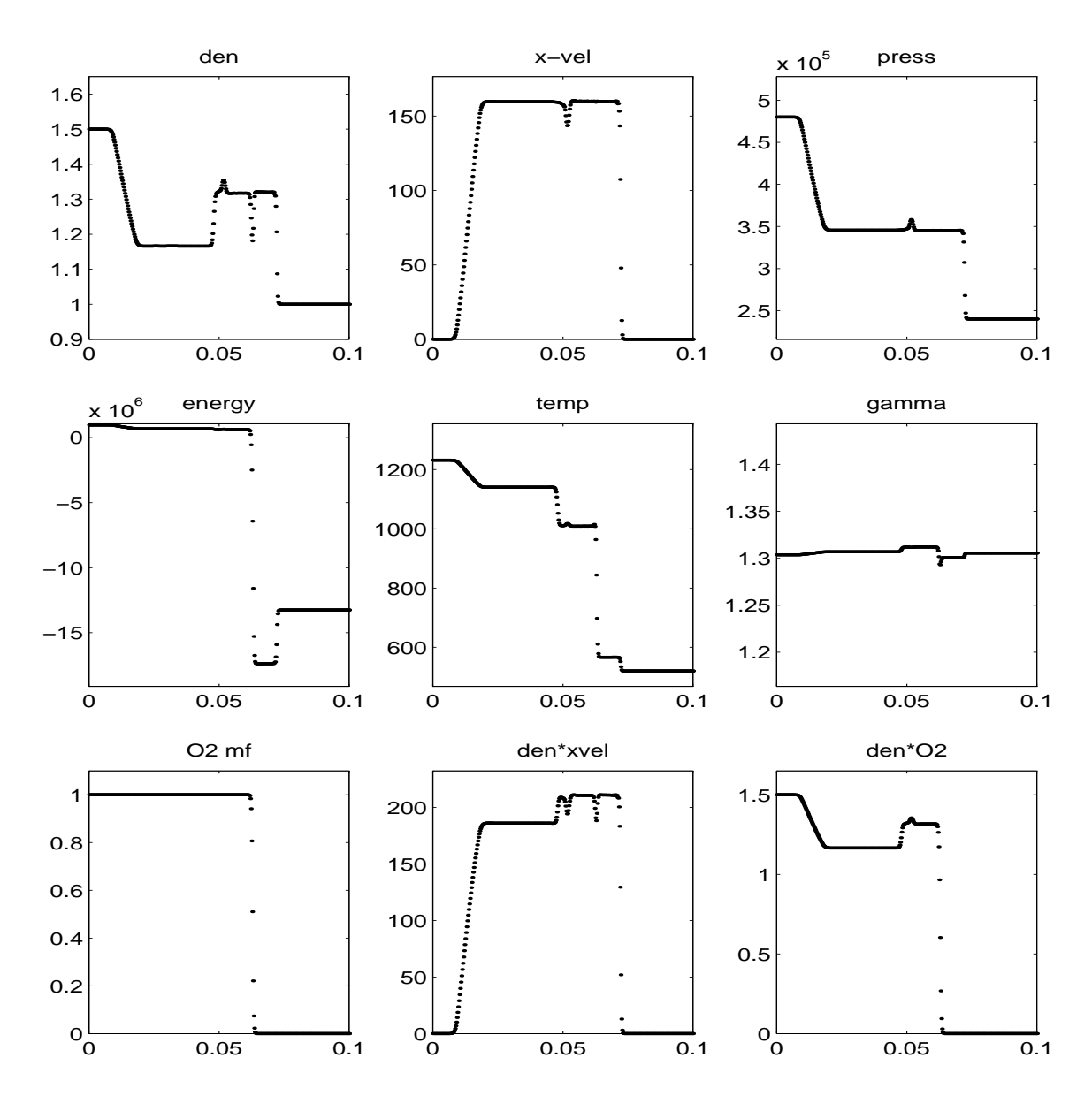


Figure 5: conservative method - after collision - 400 points

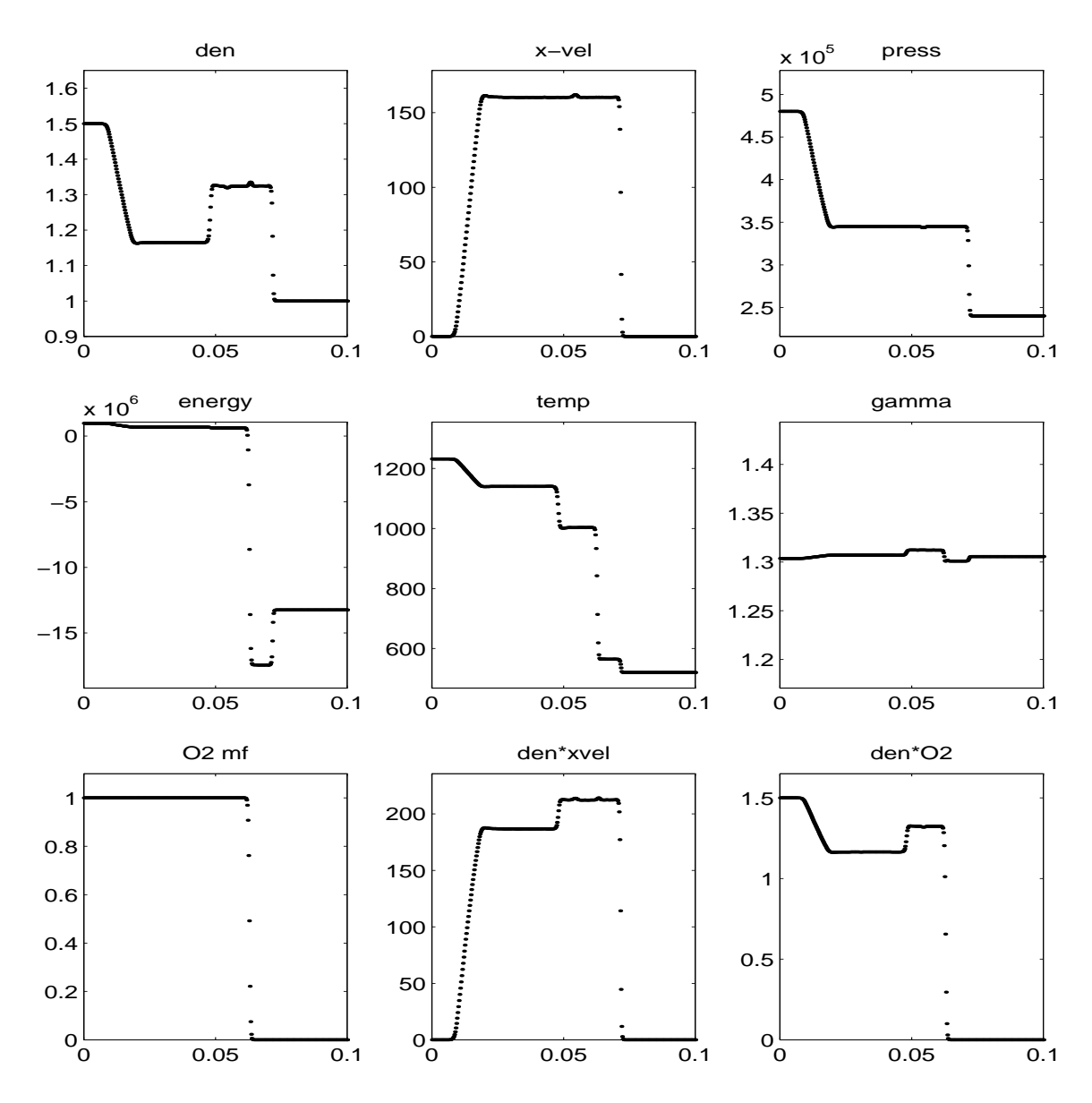


Figure 6: nonconservative correction - after collision - $400~\mathrm{points}$

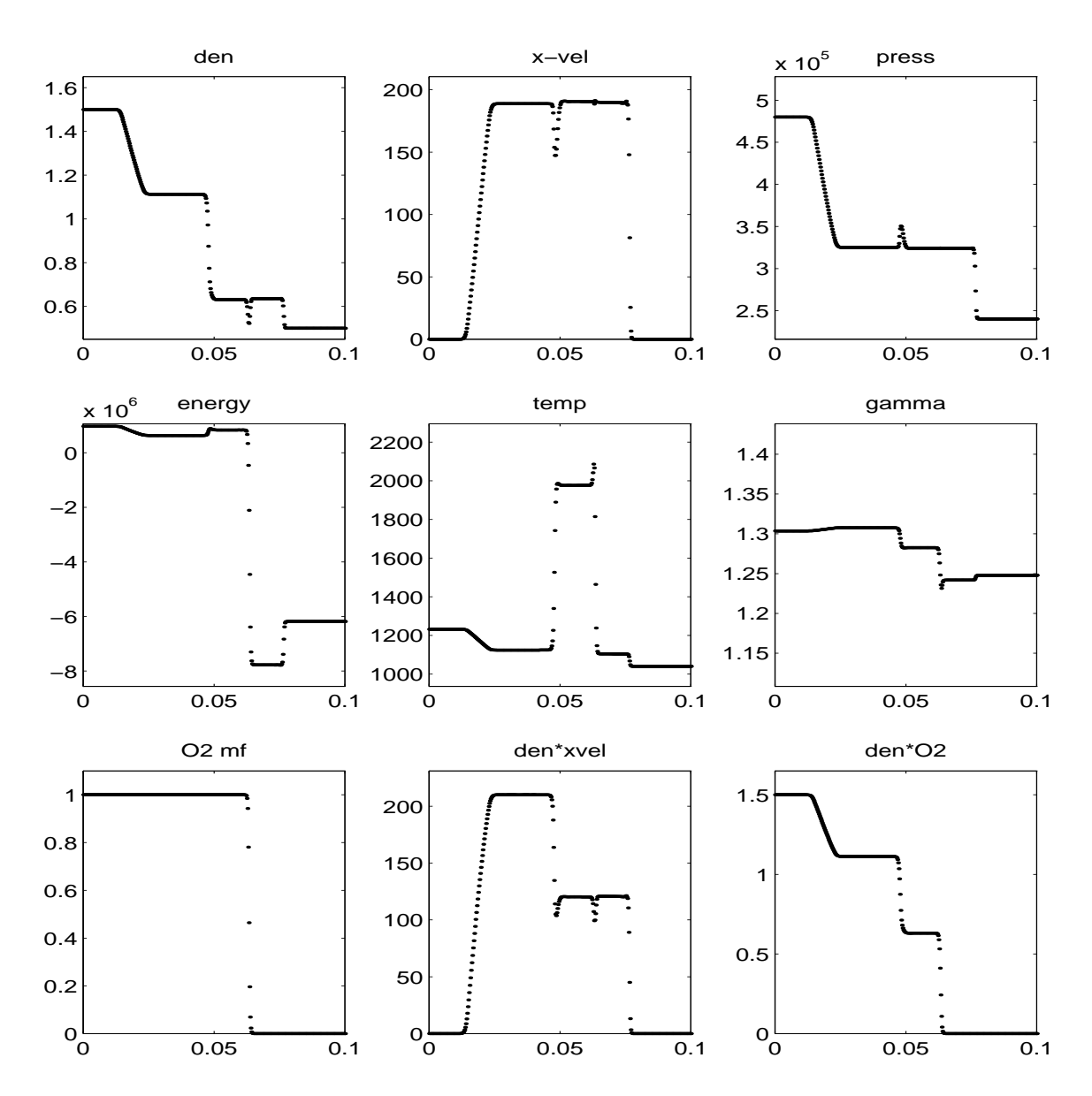


Figure 7: conservative method - after collision - 400 points

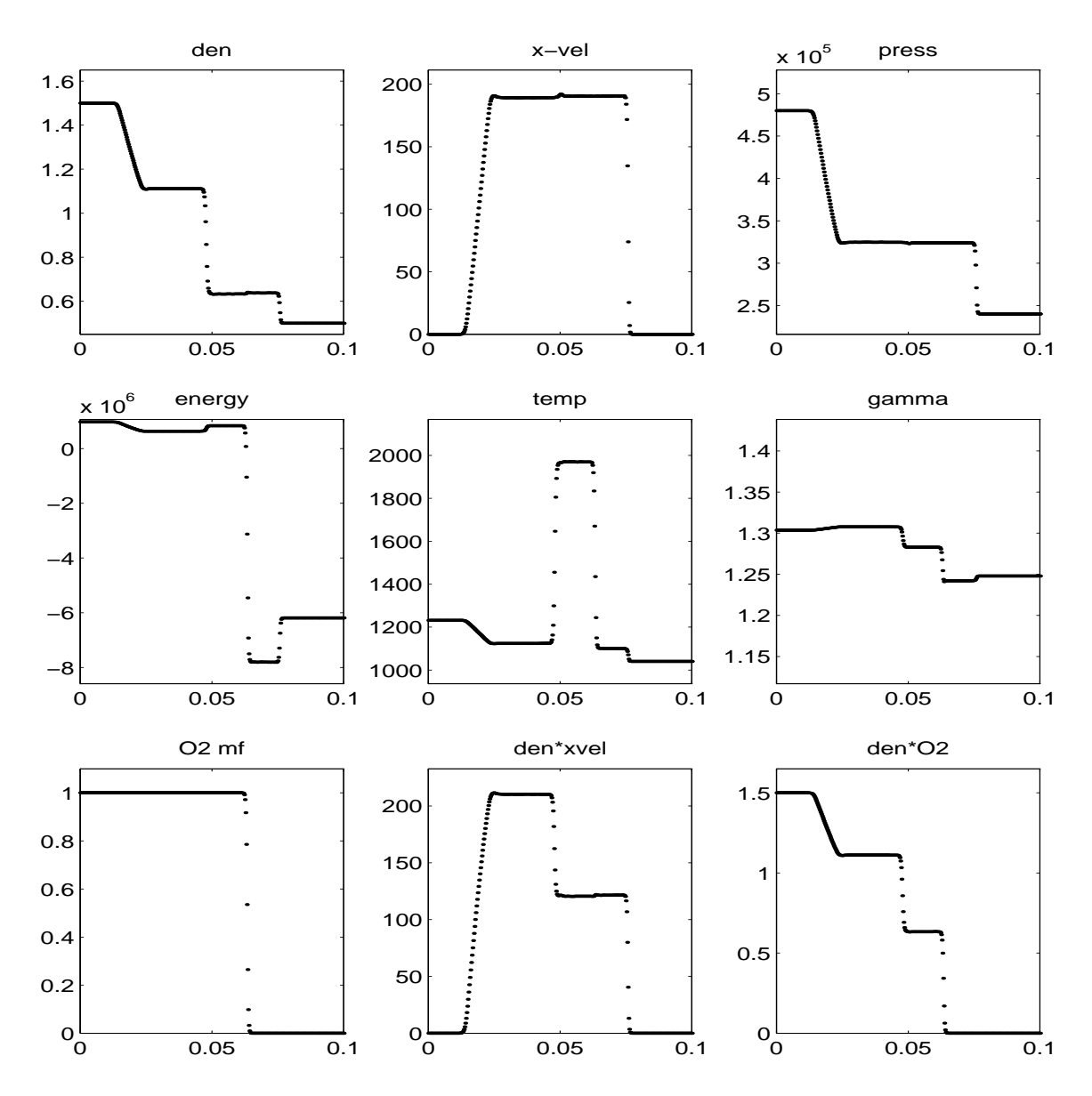


Figure 8: nonconservative correction - after collision - 400 points

6 Conclusions

In this paper, we stated and discretized the pressure evolution equation for the thermally perfect Euler equations. The solution of the pressure evolution equation was used to make a nonconservative modification of the total energy computed with a fully conservative numerical method. The numerical results imply that this nonconservative correction helps to alleviate the nonphysical oscillations present in the fully conservative numerical method.

References

- [1] Abgrall, R., How to Prevent Pressure Oscillations in Multicomponent Flow Calculations: A Quasi Conservative Approach, J. Comput. Phys. 125, 150-160 (1996).
- [2] Fedkiw, R., Merriman, B., and Osher, S., Efficient Characteristic Projection in Upwind Difference Schemes for Hyperbolic Systems (The Complementary Projection Method), J. Comput. Phys. 141, 22-36 (1998).
- [3] Fedkiw, R., Merriman, B., and Osher, S., *High Accuracy Numerical Methods for Thermally Perfect Gas Flows with Chemistry*, J. Comput. Phys. 132, 175-190 (1997).
- [4] Fedkiw, R., Merriman, B., Donat, R., and Osher, S., The Penultimate Scheme for Systems of Conservation Laws: Finite Difference ENO with Marquina's Flux Splitting, Progress in Numerical Solutions of Partial Differential Equations, Arachon, France, edited by M. Hafez, July 1998.
- [5] Jenny, P., Muller, P. and Thomann, H., Correction of Conservative Euler Solvers for Gas Mixtures, J. Comput. Phys. 132, (1997).
- [6] Karni, S., *Hybrid Multifluid Algorithms*, SIAM J. Sci. Statist. Comput. 17, 1019-1039 (1996).
- [7] Karni, S., Multicomponent Flow Calculations by a Consistent Primitive Algorithm, J. Comput. Phys. 112, 31-43 (1994).
- [8] Karni, S., Viscous Shock Profiles and Primitive Formulations, SIAM J. Numer. Anal. 29, 1592-1609 (1992).
- [9] Mulder, W., Osher, S., and Sethian, J.A., Computing Interface Motion in Compressible Gas Dynamics, J. Comput. Phys. 100, 209-228 (1992).
- [10] Saurel, R. and Abgrall, R., A Simple Method for Compressible Multifluid Flows, SIAM J. Sci. Comput. 21, 1115-1145 (1999).
- [11] Shyue, K.-M., An Efficient Shock-Capturing Algorithm for Compressible Multicomponent Problems, J. Comput. Phys. 142, 208-242 (1998).
- [12] Shyue, K.-M., A Fluid-Mixture Type Algorithm for Compressible Multicomponent Flow with Van der Waals Equation of State, J. Comput. Phys. 156, 43-99 (1999).